The ozone-climate penalty: past, present and future

By

David M. Rasmussen Jr.
B.S. UW-Madison 2009

Thesis

Submitted in partial satisfaction of the requirements for the degree of

Master of Science

in

Civil and Environmental Engineering

in the

Office of Graduate Studies

of the

University of California

Davis

Approved:

Prof. Michael J. Kleeman, Chair

Prof. Cort Anastasio

Associate Prof. Christopher D. Cappa

Committee in Charge

2013

Contents

List of Figures

Abstract of the Thesis

The ozone-climate penalty: past, present and future

Climate change is expected to exacerbate tropospheric ozone (O_3) in already heavily polluted areas. The O_3-climate penalty quantifies the increase in O_3 pollution due to an increase in temperature. Previous studies have shown a decreasing trend in the O_3-climate penalty over the past two decades over the eastern U.S. due to dramatic reductions in precursor emissions of nitrogen oxide (NO_x). However, these studies have ignored the contributing effects of evolving emissions of volatile organic compounds (VOCs) on the value of the O_3-climate penalty over the same period. Here, the UC-Davis-Caltech (UCD-CIT) air quality model is used to simulate conditions during two severe pollution episodes in California's most heavily polluted air basins, the South Coast Air Basin (SoCAB) and the San Joaquin Valley (SJV). The emissions of anthropogenic O_3 precursors during each episode to are scaled up and down to match both historical and future emission conditions while a +5 K temperature perturbation is applied to determine the O_3-climate penalty. Historical values of the O_3-climate penalty range from +8.0 ppb K^{-1} in the SoCAB and +3.0 ppb K^{-1} in the SJV in the 1980s to present day values of +2.0 ppb K^{-1} in the SoCAB and +1.5 ppb K^{-1} in the SJV in the 2000s. The UCD-CIT model well reproduces the 1980—2005 range of O_3-climate penalties from the literature that are constructed from long-term measurements of temperature and ozone as well as values from model perturbation studies (r^2=0.98 in the SoCAB; r^2=0.53 in the SJV). The 2020 median O_3-climate penalties are projected to be +0.8 ppb K^{-1} in the SoCAB and +0.7 ppb K^{-1} in the SJV, suggesting that under the current projected emissions pathway, increases in temperature due to climate change may continue to have deleterious effects on O_3 control programs. Results further indicate both reductions in NO_x and concomitant cuts of anthropogenic VOC emissions may be beneficial to abate O_3 during severe pollution events and to further diminish the O_3-climate penalty.

Acknowledgments

I would like to first and foremost acknowledge the continuing support of my adviser, Prof. Kleeman. His level of expertise is tremendous and has made finishing this project possible. I would also like to acknowledge the assistance of Dr. Jianlin Hu, Dr. Abdullah Mahmud, and Mark Hixon for the use of their data processing tools in helping finish this important project. I would also like to acknowledge my readers, Prof. Anastasio and Prof. Cappa.

Chapter 1

Introduction

Surface ozone is a secondary pollutant that is produced by the photochemical oxidation of CO and volatile organic compounds (VOCs) by hydroxyl radical (OH) in the presence of nitrogen oxide radicals ($NO_x \equiv NO_2 + NO$). Model perturbation studies have identified temperature as the most important weather variable affecting surface ozone concentrations in polluted regions (Aw and Kleeman, 2003, Dawson et al., 2007, Kleeman, 2008, Millstein and Harley, 2009, Steiner et al., 2006). These findings have been buttressed against observations on multiple time scales that have shown strong correlation between temperature and tropospheric ozone concentrations in excess of about 60 ppb (Mahmud et al., 2008, Sillman and Samson, 1995, Steiner et al., 2010). The aggregate effects that make up this relationship (the total derivative, $d[O_3]/dT$) have been thought to include at least three components:

$$\frac{d[O_3]}{dT} = \frac{\partial[O_3]}{\partial[stagnation]} * \frac{d[stagnation]}{dT} + \frac{\partial[O_3]}{\partial[AN]} * \frac{d[AN]}{dT} + \frac{\partial[O_3]}{\partial[BVOC]} * \frac{d[BVOC]}{dT} + ...$$

1) association of warm temperatures with stagnant air masses that facilitate the accumulation of ozone precursor species (Jacob et al., 1993); (2) thermal decomposition of alkyl nitrates (AN), including peroxyacetylnitrate (PAN), reservoirs for both NO_x and HO_x at low temperatures (Sillman and Samson, 1995); (3) temperature dependent variations in biogenic emissions of VOCs (BVOCs), which act as a significant source of precursors for ozone formation under high-NO_x conditions and tend to increase with temperature for many species

(Guenther et al., 1993, Harley et al., 1998). Other contributing temperature-dependent processes of varying sign have been identified (*see Jacob and Winner, (2009) and references therein*). Model perturbation studies resolve the partial derivatives, while observations ascertain the total derivative.

1.1 Future climate change in California

A warming climate is expected to exacerbate surface ozone in California's South Coast Air Basin (SoCAB) and San Joaquin Valley (SJV), currently the location of seven of the top ten most heavily ozone polluted metropolitan areas in the United States, despite the dramatic reductions of NO_x and VOC precursor emissions over the past three decades (AmericanLungAssociation, 2013, Fujita et al., 2013, Kleeman, 2008, Mahmud et al., 2008, Millstein and Harley, 2009, Parrish et al., 2011, Steiner et al., 2006, Warneke et al., 2012). The Intergovernmental Panel on Climate Change projects annual average temperatures over Western North America, including the aforementioned air basins with recalcitrant air quality, will warm between +2 to +6 K over the next century (Christensen et al., 2007), while urban "heat-island" effects may further raise the temperature in parts of megacities, such as Los Angeles, +5 K above that of surrounding regions (Diffenbaugh et al., 2008). These temperature increases may counter the benefits from pollution control technology used in an effort to meet established air quality standards, resulting in a "climate penalty" (Jacob and Winner, 2009, Wu et al., 2008). Here, the increase in ozone pollution due to increasing temperatures (ppb K^{-1}) is referred to as the "ozone-climate penalty" or "climate penalty". Previous studies have shown the past and present climate penalty to be highly varied in space and time due to differing chemical and meteorological environments that influence ozone formation (Bloomer et al., 2009, Kleeman, 2008, Mahmud et al., 2008, Millstein and Harley, 2009, Steiner et al., 2010). Extrapolation of this metric to future climate to estimate changes in ozone air quality assumes invariable emission rates and ignores complex chemistry-climate interactions (Fiore et al., 2012, Jacob and Winner, 2009, Weaver et al., 2009).

1.2 Historical trend in ozone-climate penalty in California

Fig. 1.1 shows the trend in average daily NO_x emissions in both air basins, along with the corresponding decadal trend in the climate penalty factor from previous model perturbation and observational studies. The climate penalty appears highly correlated with NO_x emissions in both the SoCAB and the SJV. From 1980 to 2010, average daily emissions of NO_x and VOCs in the SoCAB decreased roughly 2 and 4-fold, respectively, while a 1.5 and 3-fold decrease in emissions occurred in the SJV (Cox et al., 2009). The dramatic decrease in emissions is reflective of the success of California's statewide emission control programs. Over this same period, the mean value of climate penalty in the SoCAB decreased from +8.0 ppb K^{-1} in the 1980s to a present-day value of +2.7 ppb K^{-1}, while the climate penalty in the SJV decreased from a value of +2.8 ppb K^{-1} in the 1980s to a current value of +1.8 ppb K^{-1} (Bloomer et al., 2009, Steiner et al., 2010, Kleeman, 2008, Mahmud et al., 2008, Millstein and Harley, 2009). Similar NO_x-climate penalty trends have been observed elsewhere. In the eastern U.S., a 43% reduction in power plant NO_x emissions between 1995 and 2002 was shown to correspond to a 1.0 ppb K^{-1} decrease in the ozone-climate penalty (Bloomer et al., 2009, Kim et al., 2006). Over the next decade, emissions of NO_x are expected to continue to decrease in both the SoCAB and the SJV raising a question as to whether the ozone-climate penalty will effectively diminish to zero, or if a particular NO_x emissions target exists that minimizes the ozone-climate penalty.

In this study, we generate ozone isopleth diagrams with an urban to regional scale airshed model using meteorological conditions from two severe weekday pollution episodes: (1) in the SoCAB during September 7-9, 1993 (described in Fraser et al. (2000), Ying et al. (2007)) and (2) in the SJV during July 23-27, 2005. An explanation of the ozone isopleth diagram has been presented elsewhere (Seinfeld and Pandis, 2006, Sillman, 1999). To generate an ozone isopleth diagram, all episode base case NO_x and non-biogenic VOC emissions were extrapolated up (more emissions) or down (less emissions) to represent a hypothetical range of pollution control technology in each air basin. A temperature perturbation is applied to each episode to calculate a value of the climate penalty ($\partial[O_3]/\partial T$) at each NO_x and

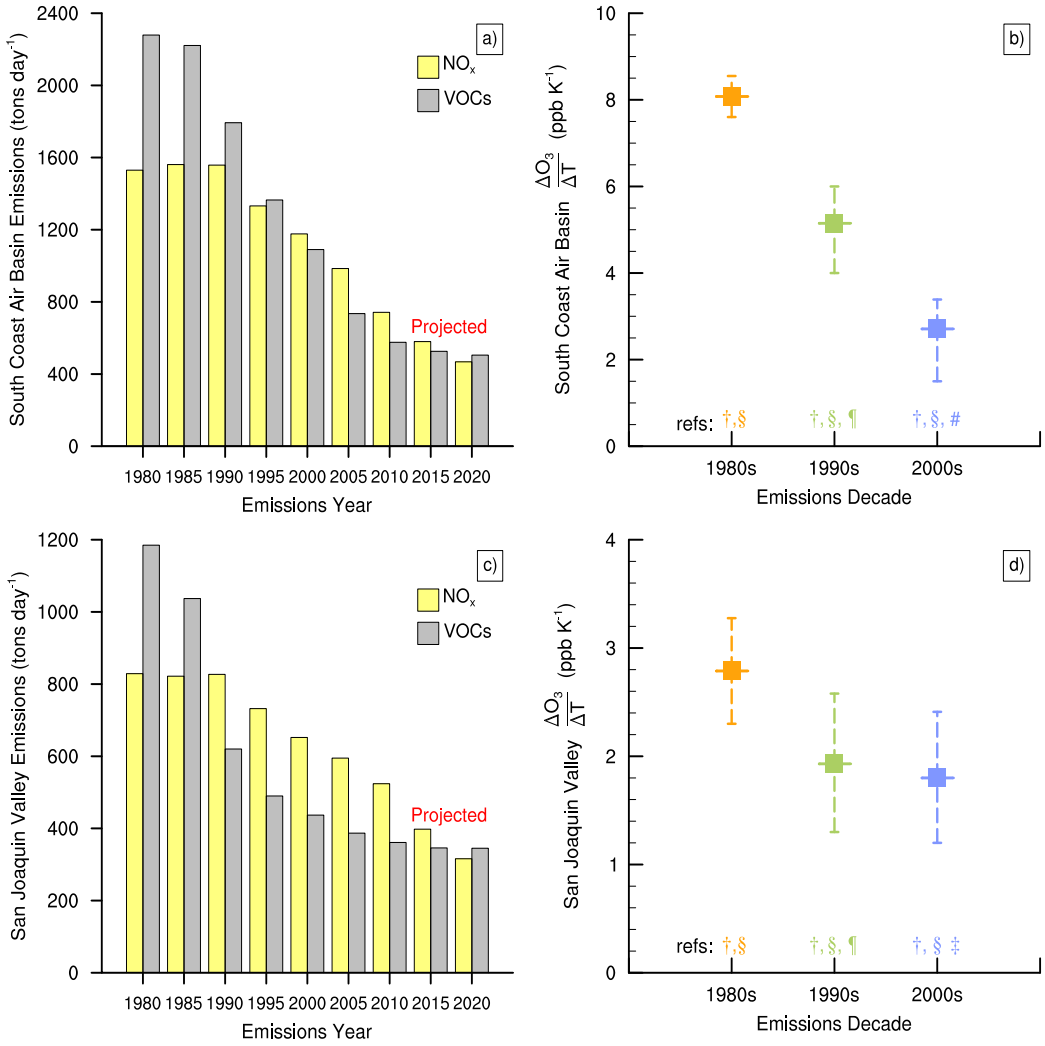

Figure 1.1. (a) Historical (black) and projected (white) average daily NO_x emissions (tons day^{-1}) versus emissions year for the South Coast Air Basin and (b) the observed decadal trend in the ozone climate penalty for the Southern California Air Basin attributed to emissions changes during the 1980s (orange), the 1990s (magenta), and the 2000s (blue). Dashed lines give the range of both observed and modeled ozone climate penalty values in the South Coast Air Basin from the literature; solid squares are the mean ozone climate penalty calculated from values given in the literature. Symbols beneath each range correspond to literature references: † is Mahmud et al., 2008 (statistical downscaling based on measured trends), § is Steiner et al., 2010 (observations), ¶ is Kleeman, 2008 (model perturbation), # is Millstein and Harley, 2009, (model perturbation), and ‡ is Steiner et al., 2006 (model perturbation); (c) as for (a) but for the San Joaquin Valley; (d) as for (b) but for the San Joaquin Valley.

VOC emissions point. With this approach, we hope to reproduce historical values of the ozone-climate penalty in each air basin. Unlike previous studies that only investigate the impacts of declining NO_x emissions on the ozone-climate penalty, we additionally wish to use

ozone-isopleth diagrams as a means to assess the behavior of the ozone-climate penalty as a function of both NO_x and VOC emissions. Finally, with the use of projected ozone precursor emissions, we hope to forecast future values of the ozone-climate penalty and determine if additional emissions controls may be needed to reduce the detrimental effects of increased temperature on ozone pollution.

Chapter 2

Methods

2.1 Model description

The UC-Davis-Caltech (UCD-CIT) air quality model is a 3D Eulerian, photochemical model that simulates reactive chemical transport in the atmosphere and predicts the concentration of both primary and secondary pollutants in the gas and particle phase. A detailed description of the UCD-CIT airshed model and its evolution has been presented previously (Kleeman and Cass, 2001, Kleeman et al., 1997, McRae et al., 1982, Mysliwiec and Kleeman, 2002, Ying et al., 2007).

Due to variations in the physical environments of each air basin, differing modeling setups were used to simulate each pollution episode. Previous studies have shown these configurations to well reproduce past conditions (Ying et al., 2007, Hu et al., 2012). Relevant chemical reactions are modeled with the SAPRC11 mechanism in the SoCAB (Carter and Heo, 2012) and the SAPRC07 mechanism in the SJV (Carter, 2010). SAPRC11 differs in its update of the aromatics mechanism; little difference in ozone production has been observed between SAPRC07 and SAPRC11 in box-model experiments (Carter and Heo, 2012). During the course of this study, SAPRC11 was introduced by the modeling community as the preferred chemical mechanism for photochemical modeling in California. The horizontal resolution used in the SoCAB simulations was 5 km $\times$ 5 km. The vertical domain was divided into 5 levels (thickness of 38.5, 115.5, 154, 363, and 429m), extending from the surface to 1.1 km above ground. The horizontal resolution in the SJV simulations was 8 km $\times$ 8 km, and the vertical distance from the surface to 5 km above ground was divided into 16 levels (thickness

of first 11 layers are 30, 30, 50, 50, 80, 80, 125, 125, 175, 175, 225m). In the SoCAB, hourly 2D and 3D meteorological fields (temperature, absolute humidity, wind speed and direction, and solar intensity) were interpolated from observations using the method described by Goodin et al. (1980, 1979), while the SJV simulations used hourly meteorological fields generated over California at 4 km × 4 km horizontal resolution with the Weather Research and Forecasting model (WRF) v3.4 (Skamarock and Klemp, 2008), driven by the North American Regional Reanalysis (NARR) (Mesinger et al., 2006). The WRF meteorological fields are downgraded to 8 km × 8 km for input to the UCD-CIT airshed model. The height of the vertical domain in the SoCAB was limited by the availability of upper level meteorological observations during the 1993 episode. A coupled online UV radiative extinction calculation accounts for the scattering and absorption of light due to high airborne particulate matter concentrations to give a more accurate representation of actinic flux.

The base case emission inventories for the SoCAB and SJV episodes were obtained from the South Coast Air Quality Management District (SCAQMD) and the California Air Resources Board (CARB) and are summarized in Griffin et al. (2002) and Ying et al. (2008), respectively. Boundary conditions at the western edge of each modeling domain were based on measured background concentrations of pollutants that are transported to California (Fraser et al., 1996, Liang et al., 1998). Modeled ozone prediction for both pollution episodes in this study had performance statistics that meet U.S. Environmental Protection Agency (EPA) guidance for air quality models (EPA, 2007).

2.2 Calculating the ozone-climate penalty

The effect of climate change on ozone formation was simulated under differing NO_x and VOC emissions rates by perturbing base case temperature fields by +5 K to determine the ozone-climate penalty, calculated here as the difference between the ozone concentrations calculated with the base case temperature profile and the base case temperature profile plus a +5 K perturbation, divided by the temperature perturbation (ppb K^{-1}). It was hypothesized that this simple approach would yield values of $\partial[O_3]/\partial T$ that are similar to $d[O_3]/dT$ calculated from long-term measurements of ozone and temperature (e.g. Rasmussen et al. (2012), Bloomer et al. (2009), Steiner et al. (2010), Mahmud et al. (2008)). Previous studies have

shown $\partial[O_3]/\partial T$ to be insensitive to the magnitude of the temperature perturbation used (Kleeman, 2008).

In this study, the temperature perturbation affects chemical kinetic reaction rates and biogenic emissions, but does not alter the evaporation of anthropogenic VOCs (Rubin et al., 2006) and is uncoupled from temperature dependent meteorological variables such as mixed layer depth, solar insolation, wind speed and wind direction because they are held constant; model perturbation studies have shown that mixed layer depth has weak positive and negative effects on ozone concentrations in polluted regions (Aw and Kleeman, 2003, Kleeman, 2008). The Clausius-Clapeyron relation predicts exponential increases in the atmospheres capacity to hold water vapor with increasing temperature. Increases in water vapor can lead to greater HO_x production, but model perturbation studies have found corresponding ozone sensitivity to be weak and the direction of the change in ozone to vary by region (Aw and Kleeman, 2003, Baertsch-Ritter et al., 2004, Dawson et al., 2007, Millstein and Harley, 2009).

Due to their distinct geographic locations, the temperature perturbations applied in the current study were applied in each air basin under differing humidity assumptions. The majority of the SoCAB is close to the Pacific Ocean where an unlimited water reservoir maintains an approximately constant RH with increasing temperature. The relative humidity (RH) was therefore held constant in the SoCAB when temperature was perturbed. In the SJV, moisture is limiting, and it is assumed absolute humidity will increase less with increasing temperature, potentially leading to a decrease in RH. Therefore, absolute humidity was held constant when applying the temperature perturbation in the SJV. Additional SJV modeling simulations that assumed constant relative humidity resulted in ozone-climate penalty values nearly identical to those that fixed absolute humidity. Biogenic emission rates of isoprene, monoterpenes, and methyl-butenol adjust to the temperature perturbation following algorithms from Guenther et al. (1993) and Harley et al. (1998).

Chapter 3

Results and Discussion

3.1 Decreases in NO_x and VOC emissions and the ozone-climate penalty response

Isopleths of 8-h. average ozone (10:00-18:00 LDT) (ppb) and ozone-climate penalty (ppb K^{-1}) for NO_x and VOC emissions rates relative to conditions on September 8-9, 1993 are shown in Fig. 3.1 at Downtown Los Angeles, Azusa, Claremont, and Anaheim. Ozone isopleth diagrams generated for Visalia, Fresno, Hanford, and Bakersfield for conditions on July 27, 2005 are shown in Fig. 3.2. Isopleth diagrams that include ozone-climate penalty for the SJV are not shown because all relevant behavior is illustrated in Fig. 3.1. Each isopleth shows the modeled base case ozone concentration under a particular set of NO_x and VOC emissions rates with the same meteorology. In these simulations, the NO_x emissions are entirely anthropogenic and the VOC emissions, while predominantly from gasoline vehicle emissions, include natural sources. The scaling factors are the fraction of NO_x and VOC emissions relative to the base years. The base year for the SJV episode is 2005 and the base year for the SoCAB episode is 1993. Base years have a scaling factor of 1.

The colors plotted on each ozone isopleth diagram in Fig. 3.1 show the magnitude of ozone-climate penalty (ppb K^{-1}). The maximum in the ozone-climate penalty occurs at a NO_x emission level slightly greater than that which produces the maximum ozone under the base case temperature simulation and at the highest VOC emission rates. This is coincident with the "ozone isopleth ridge", or the line of maximum ozone formation. The minimum in ozone-climate penalty occurs in conditions that are appreciably NO_x-saturated. The

simulations here suggest that when NO_x emissions are much greater than VOC emissions, the ozone-climate penalty may become strongly negative at Downtown LA and Anaheim (-0.14 to -0.38 ppb K^{-1}) (ozone decreases with increasing temperature), suggestive of further NO_x-saturation from the thermal decomposition of PAN at hotter temperatures (Sillman and Samson, 1995). The effect may be small, however, as PAN lifetime is effectively cut in half every 4.5K between 280-320K (Steiner et al., 2010). The hottest daily temperatures during these episodes are around 315K. A simple calculation using a temperature dependent rate constant gives a PAN lifetime of around a few minutes at this temperature. Nonetheless, over the next decade substantially NO_x-saturated conditions are not predicted by the emissions trajectory at any of the receptors in Fig. 2.

The historical and projected trend (1990—2020) in average daily NO_x and VOC emissions rates, relative to the respective base case inventory, is drawn on each isopleth diagram as black (historical) and grey (projected) dots connected by a dashed black line, taken together to constitute an emissions trajectory. Receptors in each air basin are assumed to experience an equivalent rate of NO_x and VOC emissions reductions. The ozone values along the NO_x-VOC emissions trajectory are an estimate of the maximum amount of ozone pollution that could be formed during a severe pollution event with similar meteorology.

In both air basins, the ozone isopleth diagrams suggest that NO_x-VOC emission reductions between 1990 and 2010 have been effective at abating ozone during weekday severe pollution events, especially in eastern LA and the SJV, confirming previous findings (Cox et al., 2009, Parrish et al., 2011). These reductions in ozone were possible through reductions in emissions of both NO_x and VOCs; had only NO_x emissions decreased over this 20-year period ozone may have correspondingly increased in the SoCAB. Little change in ozone is seen at both Anaheim and Downtown LA (Fig 3.1a, d). Measurements from CARB's monitoring network slightly differ from these modeled predictions.[1] Trends in the max annual 8-h. ozone at Anaheim (from nearby La Habra monitoring station) have shown decreases from 1990—2000 (140 ppb to 90 ppb); no significant trend in max annual 8-h. ozone is observed between 2000—2012 over this location. Trends in the max annual 8-h. ozone at Downtown LA have shown decreases in ozone from 1990—1994 (110 ppb to 85 ppb), but no

[1]CARB, Air Quality Trend Summaries; http://www.arb.ca.gov/adam/trends/trends1.php

significant trend in max annual 8-h. ozone is observed between 1994—2012 over Downtown LA. Additionally, all values of annual max. 8-h. ozone from CARB include weekend ozone concentrations that are known to be higher than weekday ozone values in a NO_x-saturated O_3-NO_x-VOC chemical system.

Over the next decade, CARB projects that NO_x and VOC emissions will continue to decrease in both air basins, with NO_x emissions declining more rapidly. Projections for the SoCAB indicate that this emissions trajectory may not be optimal, with slight increases in ozone concentrations (+20-30 ppb) under the meteorological conditions studied. This result is consistent with previous studies. Fujita et al. (2013) find that reductions in NO_x emissions without concurrent VOC emission reductions over the next decade will cause ozone to increase in central portions of the SoCAB during weekdays. No such effect is predicted for the SJV in the present study; the ozone isopleths for the SJV predict continued decreases in ozone over the next decade under meteorological conditions conductive to ozone formation (Fig. 3.2).

The historical and projected trend in the ozone-climate penalty can be inferred from the NO_x-VOC emission trajectory on the isopleths in Fig. 3.1. Both NO_x and VOC emissions appear to play a role in determining the ozone-climate penalty in the SoCAB, contrary to previous findings that suggest NO_x emissions are the primary explanatory variable in the observed decreasing trend in the ozone-climate penalty (Bloomer et al., 2009). The SoCAB is an urban environment that is NO_x-saturated during weekdays (Pollack et al., 2012), while both the SJV and the eastern U.S. are invariably NO_x-limited (Duncan et al., 2010). Reducing NO_x emissions, primarily emitted as nitric oxide (NO), in a NO_x-saturated environment can exacerbate ozone pollution by both decreasing ozone loss by NO titration and increasing the ratio of VOCs to NO_x. An increased VOC/NO_x ratio favors peroxy (HO_2) and alkylperoxy (RO_2) formation, both of which propagate the chain reaction mechanism that produces ozone in the troposphere (Seinfeld and Pandis, 2006). While NO_x emission controls may be effective at decreasing the ozone-climate penalty in the NO_x-limited eastern U.S. (Bloomer et al., 2009) and SJV (Duncan et al., 2010), the results of the current study suggest that further decreases in VOC emissions over the next decade in the SoCAB (NO_x-saturated) may be beneficial to reducing base case ozone pollution and may additionally be

effective at minimizing the ozone-climate penalty.

3.2 Future trend in the ozone-climate penalty in California

The ozone isopleth diagrams illustrate climate penalty-emissions relationships, but do not readily facilitate an air-basin wide assessment of historical and projected trends in the ozone-climate penalty along the emissions trajectory because they only illustrate behavior at individual receptor sites. To characterize an air-basin wide climate penalty, we use 18 urban receptor sites in the SJV and 26 urban receptor sites in the SoCAB. These receptors are shown in Fig. 3.3 and are the same receptor sites that are used by Steiner et al. (2010). Box-and-whisker plots are made using ozone-climate penalties at these receptors. Fig. 3.4 shows box-and-whisker plots of the modeled historical (1985—2010) and projected (2015—2020) trend in ozone-climate penalty (ppb K^{-1}) in the SoCAB (left) and the SJV (right).

Modeled results are presented as box-and-whisker plots (25^{th}, median, and 75^{th} percentiles) where the whiskers are the mean (not shown) $\pm$ the standard deviation. Extreme values are plotted as crosses. Historical values of the ozone-climate penalty from the literature (as both air basin averages and at individual receptors) are drawn as solid black symbols. Values given by Steiner et al. (2010) are decadal air basin averages constructed from long-term measurements and likely capture the full ozone-temperature relationship. The observed trend of the ozone-climate penalty from all literature sources are well reproduced by the air quality model (r^2=0.98 in the SoCAB; r^2=0.53 in the SJV). The median model prediction is systematically lower than the measured climate penalty from Steiner et al. (2010) by, at most, 0.8 ppb K^{-1} in the SoCAB over the past three decades, and by, at most, 0.7 ppb K^{-1} in the SJV from the 1990s to the 2000s. The 1980s ozone-climate penalty in the SJV from Steiner et al. (2010) is under-predicted by the model by roughly 1.4 ppb K^{-1}. These negative biases produced by the model may reflect emissions sector changes (i.e. changes to VOC reactivity (Pusede and Cohen (2012)) during the past three decades that are not captured using the uniform emissions scaling approach employed in the current study, or other contributions that increase climate penalty that are not captured with this study's simple temperature perturbation approach that only effects kinetic rate constants,

biogenic emission rates, and water vapor.

The range of climate penalties at receptors in the SoCAB in 1985 varies over three orders of magnitude, +0.7 ppb K^{-1} to +26.2 ppb K^{-1}, a substantially wider range of variability compared to the SJV, +0.3 ppb K^{-1} to +3.1 ppb K^{-1}. Receptors east of Los Angeles that are adjacent to the San Gabriel Mountains (a large source of biogenic VOCs) have the largest climate penalties through out the simulation period (1985—2020). These sites likely are highly sensitive to increased biogenic VOC emissions through rises in temperature. The central and coastal receptors in the SoCAB consistently have the lowest climate penalty, as they may be saturated with fresh NO emissions that titrate ozone. While the future median ozone-climate penalty is projected to decrease steadily in both air basins, some receptors in the SoCAB near the San Gabriel Mountains (e.g. Azusa and Claremont, Fig. 3.1b-c) are expected to experience a rise in the climate penalty due to the strengthening sensitivity of ozone to strong biogenic emissions in a region where NO_x decreases much more rapidly than VOC emissions. The 2020 median ozone-climate penalty is projected to be +0.8 ppb K^{-1} in the SoCAB (basin-wide range of -0.8 ppb K^{-1} to +11.8 ppb K^{-1}) and +0.7 ppb K^{-1} in the SJV (basin-wide range of -0.1 ppb K^{-1} to +1.4 ppb K^{-1}), suggesting under the projected emissions pathway, increases in temperature due to climate change may continue to have deleterious effects on ozone control programs. Although average daily NO_x and VOC emissions are projected to decrease 37% and 12%, respectively, over the next decade in the SoCAB (Cox et al., 2009), potential concomitant anthropogenic VOC emissions reductions may be beneficial to reduce both base case ozone and to further diminish the ozone-climate penalty.

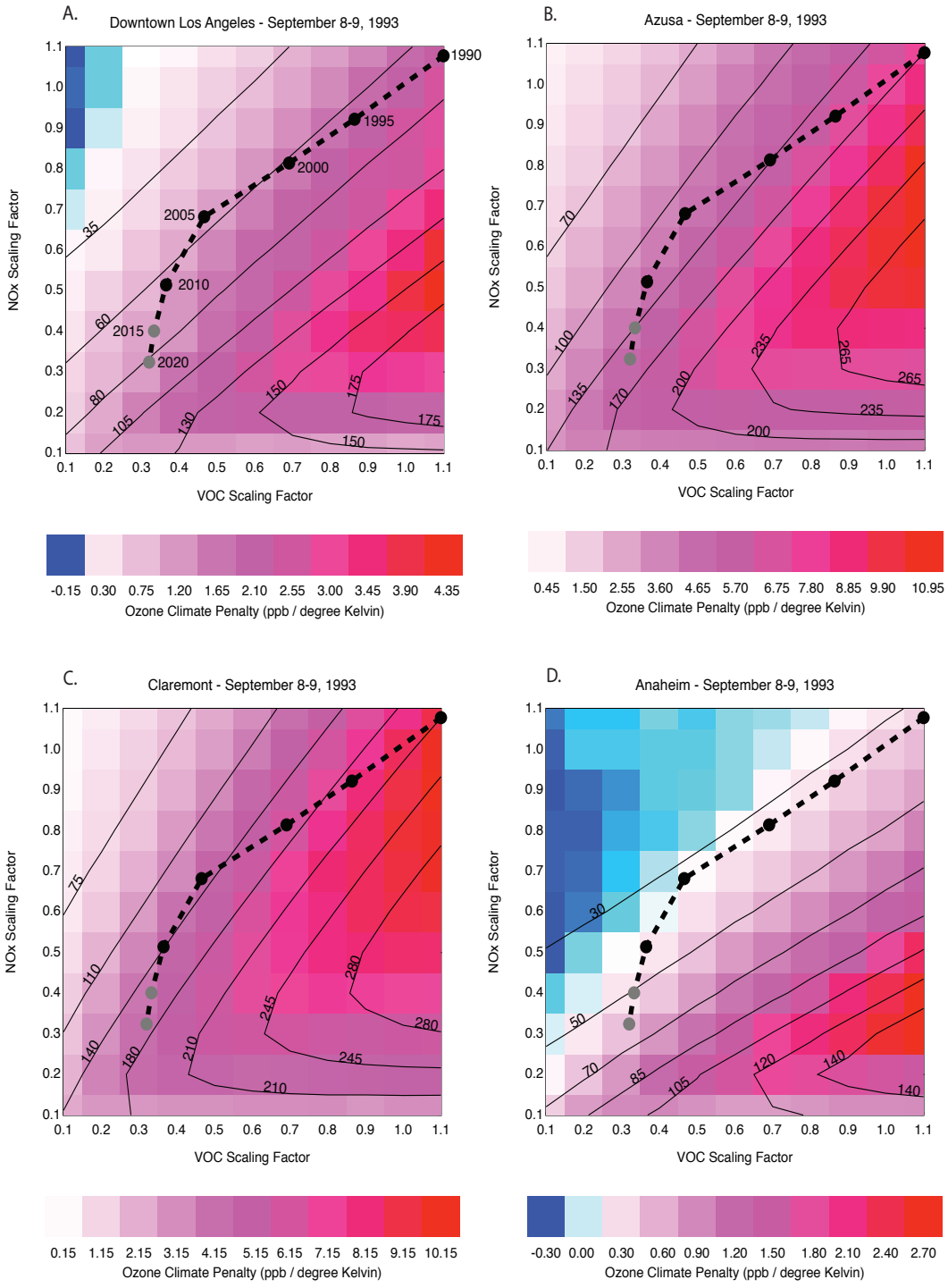

Figure 3.1. Isopleths of 8 hr. average ozone (ppb)(solid black lines) and ozone climate penalty (ppb K^{-1})(colors) generated from a 5 K temperature perturbation for (a) Downtown Los Angeles, (b) Azusa, (c) Claremont, and (d) Anaheim. All calculations are for the conditions on September 8-9, 1993. Estimated emissions trend relative to the 1993 base year is shown as a dashed black line.

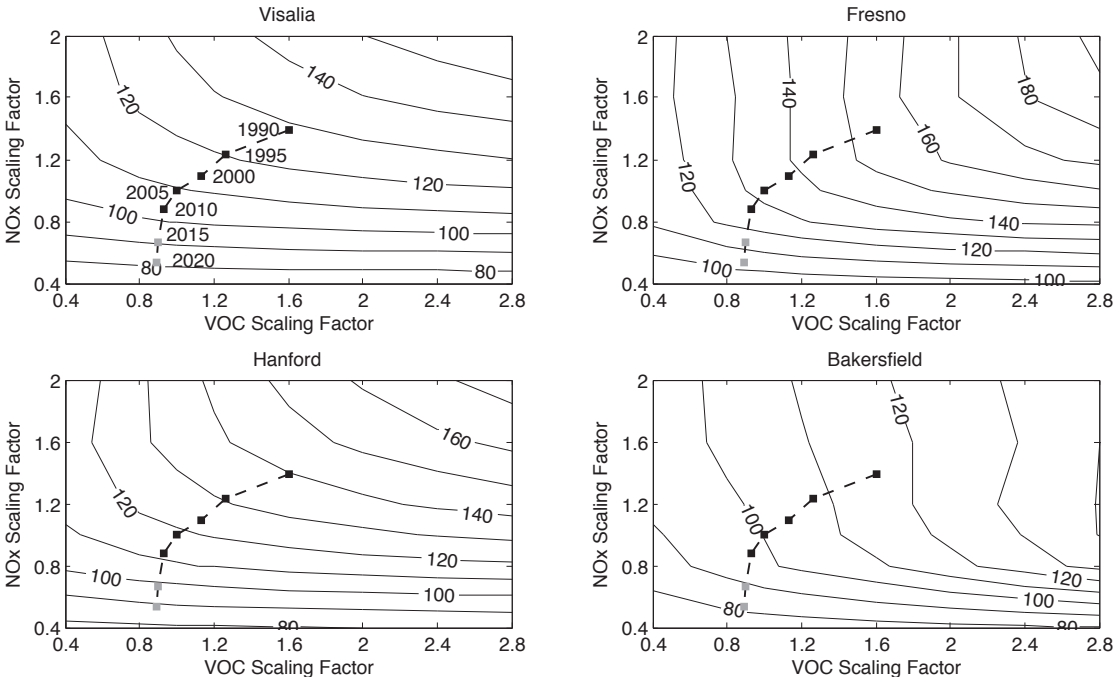

Figure 3.2. Isopleths of 1 hr. maximum ozone (ppb) for (a) Visalia, (b) Fresno, (c) Hanford, and (d) Bakersfield. All calculations are for the conditions on July 27, 2005. Estimated emissions trend relative to the 2005 base year is shown as a dashed black line. Black markers indicate historical emissions while gray markers are projected emissions.

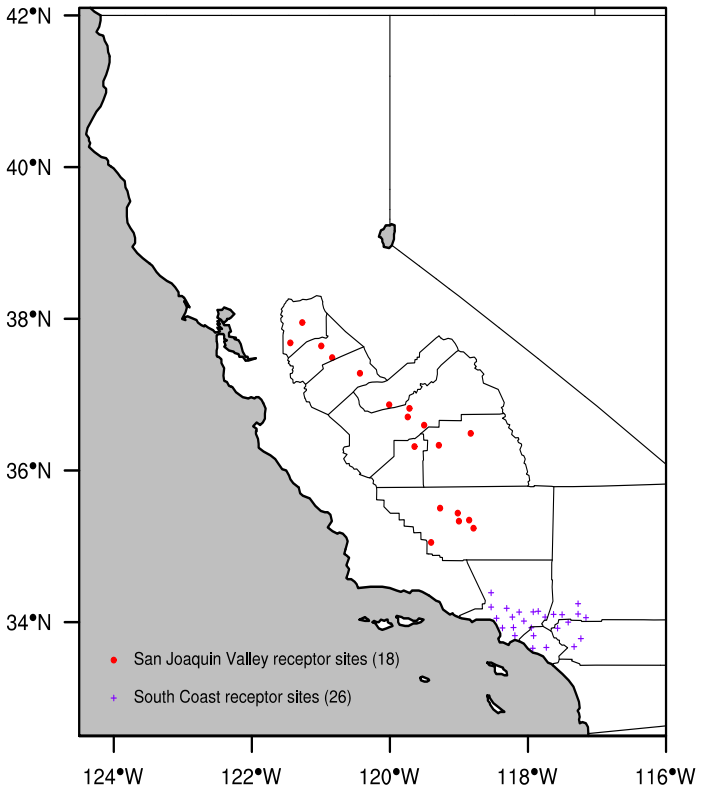

Figure 3.3. Map showing the location of the receptors in the San Joaquin Valley (red circles) and the South Coast Air Basin (purple crosses) where modeled ozone data was extracted from to generate figure 3.4

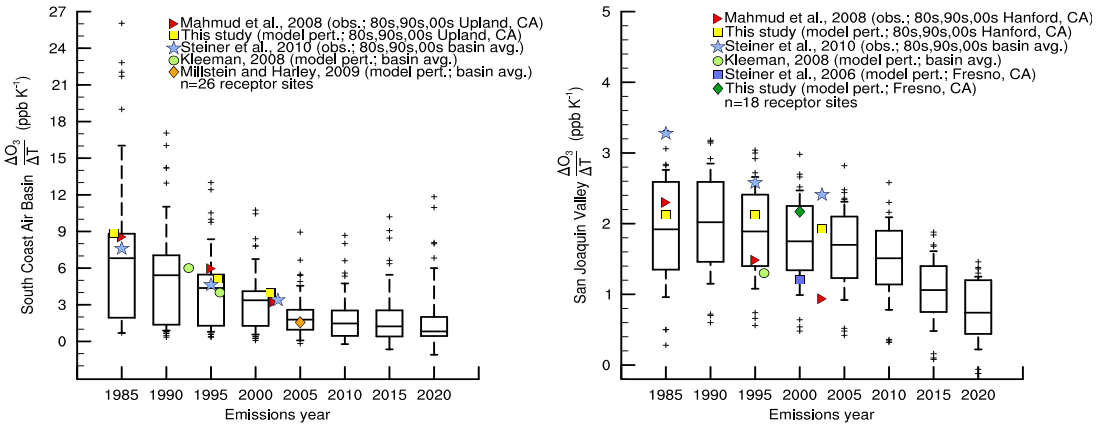

Figure 3.4. Historical (colored markers) and modeled ozone climate penalty (ppb K^{-1}) for emissions years from 1985 to 2020 for the South Coast Air Basin (SoCAB) (left) and the San Joaquin Valley Air Basin (SJV) (right). The box-and-whisker plots (mean minus the standard deviation, 25^{th}, 50^{th}, 75^{th}, and mean plus the standard deviation) give statistics of the modeled ozone climate penalty at 26 urban receptors in the South Coast Air Basin and at 18 urban receptors in the San Joaquin Valley (*see Fig. 3.3*). Values greater or less than the mean ± the standard deviation are shown as crosses. All modeled calculations are for the conditions on September 8-9, 1993 (SoCAB) and July 27, 2005 (SJV).

Chapter 4

Summary and Implications

In this study, we use the UCD-CIT air quality model to simulate conditions during two severe weekday pollution episodes: (1) in the SoCAB during September 7-9, 1993 (described in Fraser et al. (2000), Ying et al. (2007)) and (2) in the SJV during July 23-27, 2005. We generate an ozone isopleth diagram for each episode by extrapolating base case NO_x and non-biogenic VOC emissions up (more emissions) or down (less emissions) to represent a hypothetical range of pollution control technology in each air basin. A temperature perturbation is applied to each episode to calculate a value of the climate penalty at each NO_x and VOC emissions point (Section 2). We reproduce historical values of the ozone-climate penalty in each air basin (r^2=0.98 in the SoCAB; r^2=0.53 in the SJV) that are constructed from long-term measurements of ozone and temperature. We find confirm previous studies that suggest the SJV is NO_x-limited and the SoCAB is NO_x-saturated on weekdays and find that further concomitant reductions in NO_x and VOC emissions in the SoCAB are needed to further reduce base case ozone. We project that the 2020 median ozone-climate penalty will be +0.8 ppb K^{-1} in the SoCAB and +0.7 ppb K^{-1} in the SJV. Under the projected emissions pathway from CARB, increases in temperature due to climate change will likely continue to have deleterious effects on ozone control programs.

Previous studies have suggested decreases in NO_x emissions will lower the climate penalty (Bloomer et al., 2009), but this appears to only be the case in O_3-NO_x-VOC systems that are NO_x-limited. Because the SoCAB is NO_x-saturated during weekdays, we find that decreases in NO_x alone in the SoCAB will likely increase the ozone climate penalty. Over the next

decade, CARB projects that average daily NO_x and VOC emissions will decrease 37% and 12%, respectively, in the SoCAB. Further decreases in VOC emissions here are likely needed to both diminish the ozone-climate penalty and to reduce base case ozone concentrations.

References

AmericanLungAssociation. State of the air report, 2013. URL `http://www.stateoftheair.org/2012/city-rankings/most-polluted-cities.html`.

J. Aw and M. J. Kleeman. Evaluating the first-order effect of intraannual temperature variability on urban air pollution. *Journal of Geophysical Research-Atmospheres*, 108 (D12), 2003.

N. Baertsch-Ritter, J. Keller, J. Dommen, and A. S. H. Prevot. Effects of various meteorological conditions and spatial emission resolutions on the ozone concentration and ROG/NOx limitation in the milan area (i). *Atmospheric Chemistry and Physics*, 4:423–438, 2004.

B. J. Bloomer, J. W. Stehr, C. A. Piety, R. J. Salawitch, and R. R. Dickerson. Observed relationships of ozone air pollution with temperature and emissions. *Geophys. Res. Lett.*, 36(9):L09803, 2009.

W. P. L. Carter. Development of the SAPRC-07 chemical mechanism. *Atmospheric Environment*, 44(40):5324–5335, 2010.

W. P. L. Carter and G. Heo. Development of revised SAPRC aromatics mechanism. Technical report, California Air Resources Board, 2012.

J.H. Christensen, B. Hewitson, A. Busuioc, A. Chen, X. Gao, I. Held, R. Jones, R.K. Kolli, W.-T. Kwon, R. Laprise, V. Magaa Rueda, L. Mearns, C.G. Menndez, J. Risnen, A. Rinke, A. Sarr, and P. Whetton. *Regional Climate Projections*. Cambridge University Press, Cambridge, United Kingdom and New York, NY, USA, 2007.

P. Cox, A. Delao, A. Komorniczak, and A. Weller. The California Almanac of Emissions and Air Quality 2009 edition, 14-08-12 2009.

J. P. Dawson, P. J. Adams, and S. N. Pandis. Sensitivity of ozone to summertime climate in the eastern USA: A modeling case study. *Atmospheric Environment*, 41(7):1494–1511, 2007.

N. S. Diffenbaugh, F. Giorgi, and J. S. Pal. Climate change hotspots in the united states. *Geophysical Research Letters*, 35(16), 2008.

B. N. Duncan, Y. Yoshida, J. R. Olson, S. Sillman, R. V. Martin, L. Lamsal, Y. Hu, K. E. Pickering, C. Retscher, D. J. Allen, and J. H. Crawford. Application of OMI observations to a space-based indicator of NOx and VOC controls on surface ozone formation. *Atmospheric Environment*, 44(18):2213 – 2223, 2010. ISSN 1352-2310. doi: 10.1016/j.atmosenv.2010.03.010.

U.S. EPA. Guidance on the use of models and other analyses for demonstrating attainment of air quality goals for ozone, PM2.5, and regional haze. Technical report, April 2007 2007.

A. M. Fiore, V. Naik, D. V. Spracklen, A. Steiner, N. Unger, M. Prather, D. Bergmann, P. J. Cameron-Smith, I. Cionni, W. J. Collins, S. Dalsoren, V. Eyring, G. A. Folberth, P. Ginoux, L. W. Horowitz, B. Josse, J. F. Lamarque, I. A. MacKenzie, T. Nagashima, F. M. O'Connor, M. Righi, S. T. Rumbold, D. T. Shindell, R. B. Skeie, K. Sudo, S. Szopa, T. Takemura, and G. Zeng. Global air quality and climate. *Chemical Society Reviews*, 41 (19):6663–6683, 2012.

M. P. Fraser, D. Grosjean, E. Grosjean, R. A. Rasmussen, and G. R. Cass. Air quality model evaluation data for organics. 1. Bulk chemical composition and gas/particle distribution factors. *Environmental Science and Technology*, 30(5):1731–1743, 1996.

M. P. Fraser, M. J. Kleeman, J. J. Schauer, and G. R. Cass. Modeling the atmospheric concentrations of individual gas-phase and particle-phase organic compounds. *Environmental Science and Technology*, 34(7):1302–1312, 2000.

J. D. Fuentes, M. Lerdau, R. Atkinson, D. Baldocchi, J. W. Bottenheim, P. Ciccioli, B. Lamb, C. Geron, L. Gu, A. Guenther, T. D. Sharkey, and W. Stockwell. Biogenic hydrocarbons in the atmospheric boundary layer: A review. *Bulletin of the American Meteorological Society*, 81(7):1537–1575, 2000.

E. M. Fujita, D. E. Campbell, W. R. Stockwell, and D. R. Lawson. Past and future ozone trends in California's south coast air basin: Reconciliation of ambient measurements with past and projected emission inventories. *Journal of the Air and Waste Management Association*, 63(1):54–69, 2013.

W. R. Goodin, G. J. McRae, and J. H. Seinfeld. A comparison of interpolation methods for sparse data: Application to wind and concentration fields. *Journal of Applied Meteorology*, 18(6):761–771, 1979. doi: 10.1175/1520-0450(1979)018⟨0761:ACOIMF⟩2.0.CO;2.

W. R. Goodin, G. J. McRae, and J. H. Seinfeld. An objective analysis technique for constructing three-dimensional urban-scale wind fields. *Journal of Applied Meteorology*, 19 (1):98–108, 1980. doi: 10.1175/1520-0450(1980)019⟨0098:AOATFC⟩2.0.CO;2.

R. J. Griffin, D. Dabdub, M. J. Kleeman, M. P. Fraser, G. R. Cass, and J. H. Seinfeld. Secondary organic aerosol - 3. urban/regional scale model of size- and composition-resolved aerosols. *Journal of Geophysical Research-Atmospheres*, 107(D17), 2002.

A. B. Guenther, P. R. Zimmerman, P. C. Harley, R. K. Monson, and R. Fall. Isoprene and monoterpene emission rate variability - model evaluations and sensitivity analyses. *Journal of Geophysical Research-Atmospheres*, 98(D7):12609–12617, 1993.

P. Harley, V. Fridd-Stroud, J. Greenberg, A. Guenther, and P. Vasconcellos. Emission of 2-methyl-3-buten-2-ol by pines: A potentially large natural source of reactive carbon to the atmosphere. *Journal of Geophysical Research-Atmospheres*, 103(D19):25479–25486, 1998.

J. Hu, C. J. Howard, F. Mitloehner, P. G. Green, and M. J. Kleeman. Mobile source and livestock feed contributions to regional ozone formation in central california. *Environmental Science and Technology*, 46(5):2781–2789, 2012. doi: 10.1021/es203369p.

D. J. Jacob and D. A. Winner. Effect of climate change on air quality. *Atmospheric Environment*, 43(1):51–63, 2009.

D. J. Jacob, J. A. Logan, R. M. Yevich, G. M. Gardner, C. M. Spivakovsky, S. C. Wofsy, J. W. Munger, S. Sillman, M. J. Prather, M. O. Rodgers, H. Westberg, and P. R. Zimmerman. Simulation of summertime ozone over North America. *Journal of Geophysical Research-Atmospheres*, 98(D8):14797–14816, 1993.

S. W. Kim, A. Heckel, S. A. McKeen, G. J. Frost, E. Y. Hsie, M. K. Trainer, A. Richter, J. P. Burrows, S. E. Peckham, and G. A. Grell. Satellite-observed us power plant NOx emission reductions and their impact on air quality. *Geophysical Research Letters*, 33(22), 2006.

M. J. Kleeman. A preliminary assessment of the sensitivity of air quality in California to global change. *Climatic Change*, 87:S273–S292, 2008.

M. J. Kleeman, G. R. Cass, and A. Eldering. Modeling the airborne particle complex as a source-oriented external mixture. *Journal of Geophysical Research: Atmospheres*, 102 (D17):21355–21372, 1997. doi: 10.1029/97JD01261.

M.J. Kleeman and G.R. Cass. A 3D Eulerian source-oriented model for an externally mixed aerosol. *Environ Sci Technol*, 35(24):4834–48, 2001.

J. Liang, L. W. Horowitz, D. J. Jacob, Y. Wang, A. M. Fiore, J. A. Logan, G. M. Gardner, and J. W. Munger. Seasonal budgets of reactive nitrogen species and ozone over the United States, and export fluxes to the global atmosphere. *J. Geophys. Res.*, 103(D11): 13435–13450, 1998.

A. Mahmud, M. Tyree, D. Cayan, N. Motallebi, and M. J. Kleeman. Statistical downscaling of climate change impacts on ozone concentrations in California. *J. Geophys. Res.*, 113 (D21):D21103, 2008.

G. J. McRae, W. R. Goodin, and J. H. Seinfeld. Development of a second-generation mathematical model for urban air pollution1. model formulation. *Atmospheric Environment*, 16(4):679 – 696, 1982. doi: 10.1016/0004-6981(82)90386-9.

F. Mesinger, G. DiMego, E. Kalnay, K. Mitchell, P. C. Shafran, W. Ebisuzaki, D. Jovic, J. Woollen, E. Rogers, E. H. Berbery, M. B. Ek, Y. Fan, R. Grumbine, W. Higgins, H. Li, Y. Lin, G. Manikin, D. Parrish, and W. Shi. North American Regional Reanalysis. *Bulletin of the American Meteorological Society*, 87(3):343–+, 2006.

D. E. Millstein and R. A. Harley. Impact of climate change on photochemical air pollution in southern California. *Atmospheric Chemistry and Physics*, 9(11):3745–3754, 2009.

M. J. Mysliwiec and M. J. Kleeman. Source apportionment of secondary airborne particulate matter in a polluted atmosphere. *Environmental Science and Technology*, 36:5376 – 5384, 2002.

D. D. Parrish, H. B. Singh, L. Molina, and S. Madronich. Air quality progress in North Nmerican megacities: A review. *Atmospheric Environment*, 45(39):7015–7025, 2011.

I. B. Pollack, T. B. Ryerson, M. Trainer, D. D. Parrish, A. E. Andrews, E. L. Atlas, D. R. Blake, S. S. Brown, R. Commane, B. C. Daube, J. A. de Gouw, W. P. Dub, J. Flynn, G. J. Frost, J. B. Gilman, N. Grossberg, J. S. Holloway, J. Kofler, E. A. Kort, W. C. Kuster, P. M. Lang, B. Lefer, R. A. Lueb, J. A. Neuman, J. B. Nowak, P. C. Novelli, J. Peischl, A. E. Perring, J. M. Roberts, G. Santoni, J. P. Schwarz, J. R. Spackman, N. L. Wagner, C. Warneke, R. A. Washenfelder, S. C. Wofsy, and B. Xiang. Airborne and ground-based observations of a weekend effect in ozone, precursors, and oxidation products in the California South Coast Air Basin. *Journal of Geophysical Research: Atmospheres*, 117(D21):, 2012. doi: 10.1029/2011JD016772.

S. E. Pusede and R. C. Cohen. On the observed response of ozone to no$_x$ and voc reactivity reductions in San Joaquin Valley California 1995 to present. *Atmospheric Chemistry and Physics*, 12(18):8323–8339, 2012. doi: 10.5194/acp-12-8323-2012.

D. J. Rasmussen, A. M. Fiore, V. Naik, L. W. Horowitz, S. J. McGinnis, and M. G. Schultz. Surface ozone-temperature relationships in the eastern US: A monthly climatology for evaluating chemistry-climate models. *Atmospheric Environment*, 47:142–153, 2012.

J. I. Rubin, A. J. Kean, R. A. Harley, D. B. Millet, and A. H. Goldstein. Temperature dependence of volatile organic compound evaporative emissions from motor vehicles. *Journal of Geophysical Research-Atmospheres*, 111(D3), 2006.

J. H. Seinfeld and S. N. Pandis. *Atmospheric chemistry and physics : from air pollution to climate change*. J. Wiley, Hoboken, N.J., 2nd edition, 2006.

S. Sillman. The relation between ozone, NOx and hydrocarbons in urban and polluted rural environments. *Atmospheric Environment*, 33(12):1821–1845, 1999.

S. Sillman and F. J. Samson. Impact of temperature on oxidant photochemistry in urban, polluted rural and remote environments. *Journal of Geophysical Research-Atmospheres*, 100(D6):11497–11508, 1995.

W. C. Skamarock and J. B. Klemp. A time-split nonhydrostatic atmospheric model for weather research and forecasting applications. *Journal of Computational Physics*, 227(7): 3465–3485, 2008.

A. L. Steiner, S. Tonse, R. C. Cohen, A. H. Goldstein, and R. A. Harley. Influence of future climate and emissions on regional air quality in California. *J. Geophys. Res.*, 111(D18): D18303, 2006.

A. L. Steiner, A. J. Davis, S. Sillman, R. C. Owen, A. M. Michalak, and A. M. Fiore. Observed suppression of ozone formation at extremely high temperatures due to chemical and biophysical feedbacks. *Proceedings of the National Academy of Sciences*, 107(46): 19685–19690, 2010.

C. Warneke, J. A. de Gouw, J. S. Holloway, J. Peischl, T. B. Ryerson, E. Atlas, D. Blake, M. Trainer, and D. D. Parrish. Multiyear trends in volatile organic compounds in Los Angeles, California: Five decades of decreasing emissions. *Journal of Geophysical Research-Atmospheres*, 117, 2012.

C. P. Weaver, E. Cooter, R. Gilliam, A. Gilliland, A. Grambsch, D. Grano, B. Hemming, S. W. Hunt, C. Nolte, D. A. Winner, X-Z. Liang, J. Zhu, M. Caughey, K. Kunkel, J-T. Lin, Z. Tao, A. Williams, D. J. Wuebbles, P. J. Adams, J. P. Dawson, P. Amar, S. He, J. Avise, J. Chen, R. C. Cohen, A. H. Goldstein, R. A. Harley, A. L. Steiner, S. Tonse, A. Guenther, J-F. Lamarque, C. Wiedinmyer, W. I. Gustafson, L. R. Leung, C. Hogrefe, H-C. Huang, D. J. Jacob, L. J. Mickley, S. Wu, P. L. Kinney, B. Lamb, N. K. Larkin, D. McKenzie, K-J. Liao, K. Manomaiphiboon, A. G. Russell, E. Tagaris, B. H. Lynn, C. Mass, E. Salath, S. M. O'neill, S. N. Pandis, P. N. Racherla, C. Rosenzweig, and J-H. Woo. A preliminary synthesis of modeled climate change impacts on U.S. regional ozone concentrations. *Bulletin of the American Meteorological Society*, 90(12):1843–1863, 2009.

S. Wu, L. J. Mickley, E. M. Leibensperger, D. J. Jacob, D. Rind, and D. G. Streets. Effects of 2000-2050 global change on ozone air quality in the United States. *J. Geophys. Res.*, 113(D6):D06302, 2008.

Q. Ying, M. P. Fraser, R. J. Griffin, J. Chen, and M. J. Kleeman. Verification of a source-oriented externally mixed air quality model during a severe photochemical smog episode. *Atmospheric Environment*, 41(7):1521 – 1538, 2007. doi: 10.1016/j.atmosenv.2006.10.004.

Q. Ying, J. Lu, A. Kaduwela, and M. J. Kleeman. Modeling air quality during the California regional PM10/PM2.5 air quality study (CRPAQS) using the UCD/CIT source oriented air quality model part II. regional source apportionment of primary airborne particulate matter. *Atmospheric Environment*, 42(39):8967–8978, 2008.